Frequency dependence of photoelectron angular distributions in small Na clusters

P. Wopperer,[1,2] P. M. Dinh,[1,2] E. Suraud,[1,2] and P.-G. Reinhard[3]
[1]*Université de Toulouse, UPS, Laboratoire de Physique Théorique, IRSAMC, F-31062 Toulouse Cedex, France*
[2]*CNRS, UMR5152, F-31062 Toulouse Cedex, France*
[3]*Institut für Theoretische Physik, Universität Erlangen, Staudtstrasse 7, D-91058 Erlangen, Germany*
(Received 18 October 2011; published 17 January 2012)

We investigate from a theoretical perspective photoelectron angular distributions (PADs) in small Na clusters in relation to recently available experimental results. We consider various (increasingly refined) levels of theory in order to better understand relevant physical trends. It is found that PADs are extremely sensitive to all details of the modeling such that a detailed description of the final state and the ionic background is necessary. Finally, we compare the theoretical description with recent experimental data on the cluster anion Na_7^- and find a satisfying agreement for full time-dependent local-density approximation (TDLDA) with ionic background.

DOI: 10.1103/PhysRevA.85.015402 PACS number(s): 33.80.Eh, 36.40.Mr, 36.40.Vz, 36.40.Wa

Photoabsorption measurements are a key tool for analyzing structure and dynamics of clusters [1–3]. More information can be gathered when also resolving reaction products, especially observables from electron emission following laser irradiation, using photoelectron spectroscopy (PES), which maps the kinetic energy of the emitted electrons [4], and photoelectron angular distributions (PADs), which give insight into the spatial structure of the emission pattern. Combined measurements of PES and PAD, which provide particularly rich information, have been done recently on metal clusters [5–9] and C_{60} [10].

The theoretical description of PAD is often based on perturbation theory [11], which is applicable to atoms [4,12] and molecules [13], but it requires good knowledge of continuum states of outgoing electrons, which makes it too involved for clusters without any symmetry. Many-body approaches for the calculation of PAD in metal clusters also exist (see, for example, [14,15]), but these are based on a jellium approximation, which may become too rough for PES and PAD. It was shown that the ionic background disturbs the electronic structure, thus affecting PES [16] and PAD [17]. A detailed, flexible, and theoretically well-founded description of PAD is thus compulsory in order to properly analyze the variety of experimental data. For example, PAD, and especially its dependence on laser frequency, cannot be fully explained with simplified models [9].

A versatile tool to describe the dynamics of molecules and clusters is provided by time-dependent density-functional theory at the level of the time-dependent local-density approximation (TDLDA). This allows for a detailed simulation of the laser excitation process also in the nonlinear regime. PES and PAD can be computed when employing absorbing boundary conditions [17,18]. Free systems constitute an ensemble of randomly oriented molecules or clusters, which requires orientation averaging. In previous work, we have proposed an efficient scheme for orientation averaging and applied it to PAD in Na clusters [19,20]. This paper is devoted to a detailed study of the frequency dependence of PAD in small Na clusters. The test case Na_8 is used in various approximations. Finally, we consider the cluster anion Na_7^- for which recent experimental results exist [8] but which is numerically very demanding due to the very small ionization potential (IP) of this anion cluster.

The cross section for one-photon emission from the single-electron (s.e.) state ϕ_i is given in first-order perturbation theory as [11]

$$\frac{d\sigma_i}{d\Omega} = \frac{4\pi^2 e^2 \omega_{\rm las}}{c} |\langle \Psi_{k\vartheta\varphi} | \mathbf{e}_{\rm pol} \cdot \hat{\mathbf{r}} | \phi_i \rangle|^2, \tag{1}$$

where $\mathbf{e}_{\rm pol}$ is the direction of the laser polarization, ϕ_i is the initial s.e. state from which the electron is removed, and $\Psi_{k\vartheta\varphi}$ is an outgoing wave traveling in direction $(\vartheta\varphi)$ with wave number k. The wave number is determined by the scattering conditions. It becomes asymptotically $k = \sqrt{2m\epsilon_{\rm out}}$, where $\epsilon_{\rm out} = \epsilon_i + \omega_{\rm las}$ with ϵ_i being the s.e. energy of the initial state and $\omega_{\rm las}$ being the photon frequency. We focus here on a linearly polarized case, following experimental conditions.

The cross section (1) applies to a fixed orientation of the cluster in space. This is appropriate when considering clusters deposited on a substrate [21]. However, most PAD measurements deal with an ensemble of free, randomly orientated clusters. The orientation-averaged PAD (OA-PAD) reduces then to the very simple form [19,20]

$$\frac{d\overline{\sigma}_i}{d\Omega} \propto 1 + \beta_2^{(i)} P_2(\cos\vartheta), \tag{2}$$

where P_2 is the Legendre polynomial of second order. $\beta_2^{(i)}$ is called the anisotropy parameter. Its value ranges between -1 and 2, if one considers exclusively one-photon processes: $\beta_2^{(i)} = 2$ corresponds to a $\cos^2\vartheta$ shape which is aligned with the laser polarization and $\beta_2^{(i)} = -1$ yields a $\sin^2\vartheta$ shape perpendicular to the laser polarization.

Cluster dynamics is described by TDLDA [22–24] using the exchange-correlation functional of [25] augmented with an averaged self-interaction correction (SIC) [26] and absorbing boundary conditions [27–29]. The coupling to the ions is mediated by soft local pseudopotentials [30]. For schematic explorations, we also consider a smooth spherical jellium model [31] for which orientation averaging is not needed.

One of the major difficulties in a perturbative description of PAD is to account properly for the outgoing wave $\Psi_{k\vartheta\varphi}$. We take Na_8 as test case and exploit the simple spherical jellium model to investigate the impact of approximations to $\Psi_{k\vartheta\varphi}$ on PAD. Spherical symmetry allows us to compute the continuum wave at any level of approximation and to compute

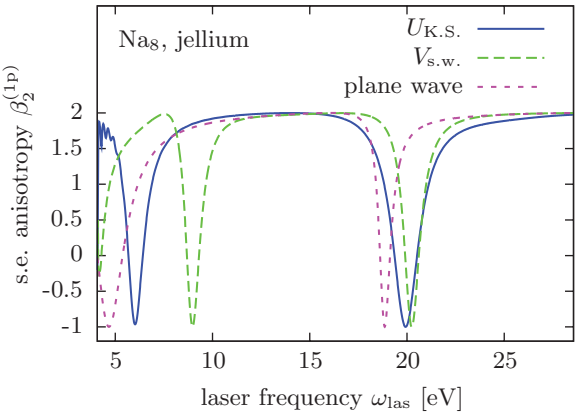

FIG. 1. (Color online) Asymmetry parameter $\beta_2^{(1p)}$ for the p shell in Na_8 in one-photon perturbation theory, as a function of laser frequency. The initial wave function was taken from a (spherical) jellium (LDA-SIC) calculation. The Wigner-Seitz radius was $r_s = 3.65\,a_0$ and the surface thickness $\sigma = 1\,a_0$. For the final wave function, continuum states has been calculated in three different scattering potentials.

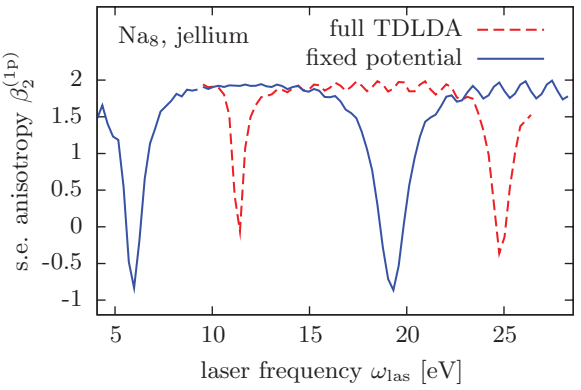

FIG. 2. (Color online) Asymmetry parameter $\beta_2^{(1p)}$ for the p shell in Na_8 with spherical jellium background, as a function of laser frequency. Compared are results obtained by full TDLDA and by TDLDA with fixed Kohn-Sham potential.

PAD directly through Eq. (1) without orientation averaging. The ground state is always calculated self-consistently with local-density approximation augmented by a SIC (LDA-SIC). For the outgoing wave $\Psi_{k\vartheta\varphi}$, we consider three cases: (1) a free plane wave, (2) a continuum wave moving in a spherical square-well potential $V_{\text{s.w.}}$, and finally (3) a continuum wave moving in the ground-state (g.s.) Kohn-Sham potential $U_{\text{K.S.}}$. Width ($8.36\,a_0$) and depth ($-6.9\,\text{eV}$) of the square-well potential were chosen so that its s.e. energies match with the s.e. energies ϵ_{1s} and ϵ_{1p} of the LDA ground state.

Figure 1 shows the frequency dependence of the asymmetry parameter $\beta_2^{(1p)}$ of the $1p$ valence electron shell for the different continuum wave functions inserted into Eq. (1). All three curves vary between -1 and 2 and show sharp minima at certain frequencies. These minima are produced by destructive interference of outgoing partial waves in the direction of the laser polarization [9]. The position of the minima, however, dramatically depends on the chosen form of the continuum wave function. The discrepancy between the three continuum models becomes even more striking for laser frequencies near the IP of $V_{i^1} = 4.08$ eV. This is reasonable because for outgoing electrons with low kinetic energy the depth of the scattering potential becomes more important than for high-energy electrons. Note that the deep minimum near threshold for the plane-wave approximation is a generic feature as can be shown analytically with Eq. (1).

The above example confirms that the continuum wave function is an essential ingredient for a correct description of PAD. The high sensitivity indicates, however, that the independent-particle picture might be a questionable assumption. Important dynamical effects in the course of the photoionization process, like polarization, rearrangement of the residual cluster, or many-body excitations, have yet to be included in the model, even if initial bound and final continuum states are calculated in the same self-consistent potential [9]. Thus, we now turn to a comparison with fully dynamical TDLDA calculations [28]. The laser excitation is described by an external field with frequency ω_{las} and a $\sin^2$ envelope of total pulse length of 60 fs, that is, an intensity FWHM of 20 fs, continuously used here. The laser intensity has to be kept low enough so that the excitation can be considered as perturbative in the one-photon domain.

In order to check the impact of dynamical rearrangement effects, we compare in Fig. 2 a fully dynamical TDLDA calculation to a TDLDA calculation in which the electrons are propagated in the frozen g.s. Kohn-Sham potential (corresponding to the perturbative treatment). The laser intensity $I = 10^{13}\,\text{W/cm}^2 \times \omega_{\text{las}}/\text{Ry}$ was scaled with the frequency in order to keep ionization in the range of 10^{-4}–10^{-1} charge units. The jellium parameters are identical to those of Fig. 1. The case with frozen Kohn-Sham potential reproduces the result of the first-order perturbation theory in Fig. 1. The full TDLDA calculation, however, yields a totally different pattern. We see that dynamic effects as the interaction of the outgoing electrons with the residual cluster have a significant influence on PAD. A full TDLDA calculation is thus required for a pertinent description of PAD.

From the above observed sensitivity of PAD, we expect that the ionic background is also very important. Thus, we have also performed TDLDA calculations using detailed ionic background. The ionic positions are frozen, which is legitimate for the short time span used here and which is necessary to stay comparable with the time-independent jellium background. Since we now deal with a nonspherical background potential, we need to apply orientation-averaging techniques to determine the OA-PAD for an ensemble of randomly orientated clusters by applying the analytical averaging procedure requiring to compute the PAD for six reference orientations [19,20]. Again, the intensity of the 60-fs laser was properly chosen to stay in the perturbative one-photon regime. The results are shown in Fig. 3.

Ionic structure breaks the strict degeneracy of the $1p$ states in Na_8 into a $1p_z$ state and two still degenerated $1p_{x,y}$ states. Nevertheless, the differences in the OA-PAD remain small. For a comparison of ionic structure and spherical jellium background, we have used two different jellium parametrizations. Jellium 1 is the same as that in Fig. 2 (Wigner-Seitz radius $r_s = 3.65\,a_0$, surface thickness $\sigma = 1\,a_0$). Jellium 2

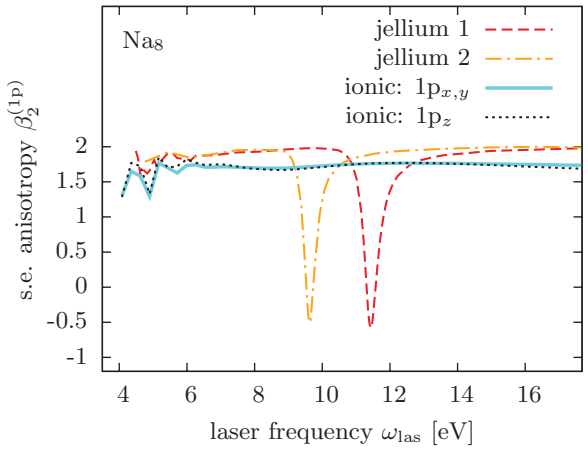

FIG. 3. (Color online) Asymmetry parameter $\beta_2^{(1p)}$ for the p states in Na_8 for two types of jellium models (jellium 1: $r_s = 3.65\,a_0$, $\sigma = 1\,a_0$; jellium 2: $r_s = 3.9\,a_0$, $\sigma = 0.7\,a_0$) and for detailed ionic structure, all calculated in TDLDA.

uses slightly different parameters ($r_s = 3.9\,a_0$, $\sigma = 0.7\,a_0$). All models deliver about the same IP (jellium 1: $V_{i^1} = 4.08$ eV; jellium 2: $V_{i^2} = 4.22$ eV; ionic background: $V_{i^{ion}} = 4.28$ eV) in accordance with the empirical value. For both jellium models, the asymmetry parameter $\beta_2^{(1p)}$ covers almost the full range of possible values between -1 and 2, as already observed previously. In contrast, the parameters for detailed ionic structure vary only little around 1.7. Particularly, the sharp minima with negative values observed in the jellium models disappear as soon as ionic structure is taken into account. For most frequencies, however, the jellium models overestimate the asymmetry parameter, which was found earlier [20]. The ionic perturbations rescatter the electronic waves and produce a sizable isotropic component. Comparing the two jellium types in Fig. 3, we observe again the great sensitivity of the PAD to small variations of the underlying potential. The frequency shift between the two minima amounts to about 1.8 eV.

We finally discuss the Na_7^- cluster, which is of particular interest since there are systematic measurements available [8]. According to our previous findings, we used fully fledged TDLDA including explicit ionic structure. The laser intensity was constantly $I = 10^9\,W/cm^2$ and the total pulse length again 60 fs. This test case is extremely demanding for the TDLDA description. The low IP of about 1.5 eV requires a huge numerical box: We are using a three-dimensional (3D) box with 160^3 mesh points and an overall box length of $280\,a_0$.

As already stressed, electronic emission is analyzed both in energy (PES) and angle (PAD). It is thus essential to account for both within the same theoretical framework. Figure 4 shows the PES for $\omega_{las} = 4.08$ eV and a fixed cluster orientation, using the techniques in Refs. [18,28,32]. The calculated s.e. energies are $\epsilon_1 = -2.82$ eV, $\epsilon_2 = -1.72$ eV, and almost degenerate $\epsilon_{3,4} = -1.43$ eV. The observed peaks match perfectly with the well-known relation $\epsilon_{out} = \epsilon_i + \nu\omega_{las}$ for a ν-photon process (here $\nu = 1$ and 2). The photoionization is dominated by one-photon processes since the two-photon peaks are substantially suppressed. The figure shows the PES parallel and perpendicular to the laser polarization. The

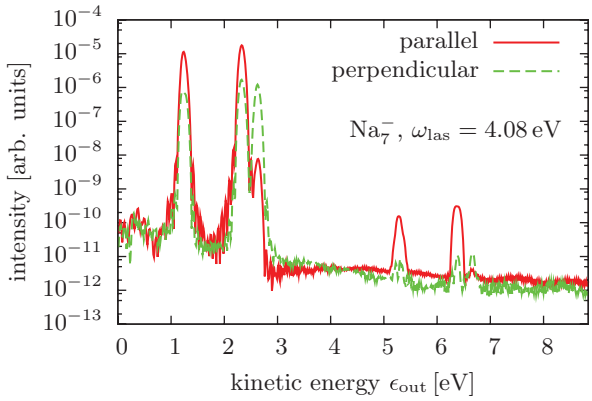

FIG. 4. (Color online) PES of the Na_7^- cluster after excitation with a laser of $\omega_{las} = 4.08$ eV, analyzed parallel (red) and perpendicular (green) to the polarization axis of the laser.

parallel direction dominates, which indicates a positive β_2 for this laser frequency.

The asymmetry parameter $\beta_2^{(1p)}$ for the $1p$ state in Na_7^- is displayed in Fig. 5 along with experimental results from [8] and calculations from [15]. The experimental data show negative values of $\beta_2^{(1p)}$ for laser frequencies closely above the IP and values around $\beta_2^{(1p)} \approx 1.5$ for higher frequencies. The TDLDA calculation (with ionic structure) reproduces this behavior very nicely. The minimum near threshold is a generic feature because the outgoing wave is almost a plane wave due to the very faint binding potential in Na_7^-. The remaining isotropic component at higher ω_{las} is a typical result for ionic structure.

We have investigated the frequency dependence of the PAD for an ensemble of small free Na clusters with isotropic distribution of orientations. The PAD has been quantified in terms of the anisotropy parameter β_2, which is the only free parameter for one-photon processes. We have compared a fully dynamical description in terms of TDLDA with traditional approaches on the grounds of one-photon perturbation theory.

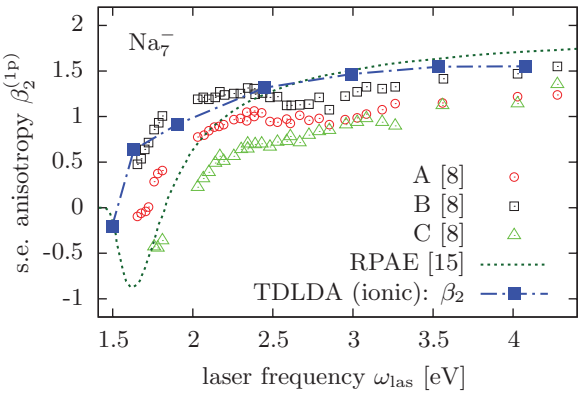

FIG. 5. (Color online) Anisotropies vs frequency for Na_7^-. Experimental results show the single-electron $\beta_2^{(1p)}$ where A, B, and C denote the different measured p states [8]. Theoretical results are total anisotropy β_2 for TDLDA results and average $\beta_2^{(1p)}$ for calculations within the random-phase approximation with exact exchange (RPAE) using spherical jellium background [15].

Considering three different models for the outgoing electron wave, we have found the PAD to be extremely sensitive to each ingredient. The choice of the outgoing waves makes dramatic differences as well as the step to the fully dynamical treatment. It becomes clear that at least full TDLDA is required for a pertinent description. Furthermore, we have compared the fully detailed ionic background with the simpler jellium background. Again, large differences are seen. In particular, the ionic structure wipes out the large fluctuations of β_2 with the frequency and produces a rather constant trend (except for a minimum near threshold for weakly bound systems). Finally, we have compared for the case of Na_7^- the results of fully ionic and fully dynamical TDLDA calculation with experimental data. The data are reproduced fairly well.

This work was supported by the Alexander von Humboldt Foundation and the Agence Nationale de la Recherche (ANR-06-BLAN-0319-02).

[1] W. A. de Heer, Rev. Mod. Phys. **65**, 611 (1993).
[2] U. Kreibig and M. Vollmer, *Optical Properties of Metal Clusters*, Springer Series in Materials Science, Vol. 25 (Springer, Berlin, 1993).
[3] H. Haberland, ed., *Clusters of Atoms and Molecules 1: Theory, Experiment, and Clusters of Atoms*, Springer Series in Chemical Physics, Vol. 52 (Springer, Berlin, 1994).
[4] P. Ghosh, *Introduction to Photoelectron Spectroscopy* (Wiley, New York, 1983).
[5] J. C. Pinaré *et al.*, Eur. Phys. J. D **9**, 21 (1999).
[6] B. Baguenard, J. C. Pinaré, C. Bordas, and M. Broyer, Phys. Rev. A **63**, 023204 (2001).
[7] O. Kostko *et al.*, J. Phys. Conf. Ser. **88**, 012034 (2007).
[8] C. Bartels, Ph.D. thesis, Albert-Ludwigs-Universität, Freiburg, 2008.
[9] C. Bartels *et al.*, Science **323**, 132 (2009).
[10] M. Kjellberg *et al.*, Phys. Rev. A **81**, 023202 (2010).
[11] F. H. M. Faisal, *Theory of Multiphoton Processes* (Plenum Press, New York, 1987).
[12] J. Cooper and R. N. Zare, J. Chem. Phys. **48**, 942 (1968).
[13] Y. Suzuki and T. Seideman, J. Chem. Phys. **122**, 234302 (2005).
[14] E. Maurat, P.-A. Hervieux, and F. Lépine, J. Phys. B **42**, 165105 (2009).
[15] A. V. Solov'yov, R. G. Polozkov, and V. K. Ivanov, Phys. Rev. A **81**, 021202(R) (2010).
[16] O. Kostko *et al.*, Eur. Phys. J. D **34** (2005).
[17] A. Pohl, P.-G. Reinhard, and E. Suraud, Phys. Rev. A **70**, 023202 (2004).
[18] A. Pohl, P.-G. Reinhard, and E. Suraud, Phys. Rev. Lett. **84**, 5090 (2000).
[19] P. Wopperer *et al.*, Phys. Lett. A **375**, 39 (2010).
[20] P. Wopperer, B. Faber, P. M. Dinh, P. G. Reinhard, and E. Suraud, Phys. Rev. A **82**, 063416 (2010).
[21] M. Bär *et al.*, Phys. Rev. B **80**, 195404 (2009).
[22] F. Calvayrac, P.-G. Reinhard, and E. Suraud, Phys. Rev. B **52**, R17056 (1995).
[23] K. Yabana and G. F. Bertsch, Phys. Rev. B **54**, 4484 (1996).
[24] F. Calvayrac, P.-G. Reinhard, and E. Suraud, Ann. Phys. (NY) **255**, 125 (1997).
[25] J. P. Perdew and Y. Wang, Phys. Rev. B **45**, 13244 (1992).
[26] C. Legrand, E. Suraud, and P.-G. Reinhard, J. Phys. B **35**, 1115 (2002).
[27] C. A. Ullrich, J. Mol. Struct., Theochem **501–502**, 315 (2000).
[28] F. Calvayrac *et al.*, Phys. Rep. **337**, 493 (2000).
[29] P.-G. Reinhard, P. D. Stevenson, D. Almehed, J. A. Maruhn, and M. R. Strayer, Phys. Rev. E **73**, 036709 (2006).
[30] S. Kümmel, M. Brack, and P.-G. Reinhard, Eur. Phys. J. D **9**, 149 (1999).
[31] B. Montag, T. Hirschmann, J. Meyer, P. G. Reinhard, and M. Brack, Phys. Rev. B **52**, 4775 (1995).
[32] P.-G. Reinhard and E. Suraud, *Introduction to Cluster Dynamics* (Wiley, New York, 2003).